SIV-induced impairment of neurovascular repair: a potential role for VEGF

Gigi J. Ebenezer · Justin C. McArthur ·
Michael Polydefkis · Jamie L. Dorsey ·
Ryan O'Donnell · Peter Hauer · Robert J. Adams ·
Joseph L. Mankowski

Abstract Peripheral nerves and blood vessels travel together closely during development but little is known about their interactions post-injury. The SIV-infected pigtailed macaque model of human immunodeficiency virus (HIV) recapitulates peripheral nervous system pathology of HIV infection. In this study, we assessed the effect of SIV infection on neurovascular regrowth using a validated excisional axotomy model. Six uninfected and five SIV-infected macaques were studied 14 and 70 days after axotomy to characterize regenerating vessels and axons. Blood vessel extension preceded the appearance of regenerating nerve fibers suggesting that vessels serve as scaffolding to guide regenerating axons through extracellular matrix. Vascular endothelial growth factor (VEGF) was expressed along vascular silhouettes by endothelial cells, pericytes, and perivascular cells. VEGF expression correlated with dermal nerve ($r=0.68$, $p=$ 0.01) and epidermal nerve fiber regrowth ($r=0.63$, $p=0.02$). No difference in blood vessel growth was observed between SIV-infected and control macaques. In contrast, SIV-infected animals demonstrated altered length, pruning and arborization of nerve fibers as well as alteration of VEGF expression. These results reinforce earlier human primate findings that vessel growth precedes and influences axonal regeneration. The consistency of these observations across human and non-human primates validates the use of the pigtailed-macaque as a preclinical model.

Keywords SIV · Blood vessel · Epidermal nerve · VEGF · Axotomy

G. J. Ebenezer · J. C. McArthur · M. Polydefkis · R. O'Donnell · P. Hauer · J. L. Mankowski
Department of Neurology, Johns Hopkins University,
Baltimore, MD 21287-7609, USA

J. L. Dorsey · R. J. Adams · J. L. Mankowski (✉)
Department of Molecular and Comparative Pathobiology,
Johns Hopkins University,
Baltimore, MD 21287, USA
e-mail: jmankows@jhmi.edu

J. C. McArthur · J. L. Mankowski
Department of Pathology, Johns Hopkins University,
Baltimore, MD 21287-7609, USA

J. C. McArthur
Department of Epidemiology, Johns Hopkins University,
Baltimore, MD 21287-7609, USA

Introduction

Numerous factors are known to influence the rate of nerve regeneration in preclinical models including the severity of injury, distance between the injury site and the innervated target, and the local milieu of the region where the nerve injury took place. The biological and physiological factors that guide these regenerating fibers are still incompletely understood. Nerves and blood vessels form well-organized networks in tissues and often project long distances to reach their target. In addition to close morphological approximation, nerves and blood vessels share an overlapping repertoire of growth factors and signals for purposes of proliferation, spatial patterning, and migration (Bates et al. 2003; Bates and Jones 2003; Carmeliet and Tessier-Lavigne 2005). Regenerating nerves rely on response to various neurotrophic factors for their outgrowth and survival (Anton et al. 1994; Griffin and Thompson 2008; Song et al. 2006; Terenghi 1999). Vascular endothelial growth factor (VEGF), a mitogen for endothelial cells in angiogenesis, is now also

considered to have neuroprotective, neurotropic, and neurogenesis functions (Brockington et al. 2006; Ferrara and Davis-Smyth 1997; Gora-Kupilas and Josko 2005; Gu et al. 2002, 2003; Jin et al. 2002; Soker et al. 2002; Sondell et al. 2000). Despite significant progress in understanding peripheral nerve regeneration using experimental rodents (Navarro et al. 2007; Saxena and Caroni 2007), axonal regeneration extending to the denervated target is a much slower and incomplete process in humans (Gordon et al. 2009; Rajan et al. 2003).

One common neurological complication associated with human immunodeficiency virus (HIV) infection is impaired axonal regeneration (Hahn et al. 2007; Polydefkis et al. 2002) that is hypothesized to potentiate axonal degeneration and ultimately development of HIV-associated sensory neuropathy (HIV-SN). The factors that contribute to impede peripheral nerve regeneration in HIV-SN remain unclear. The SIV/pigtailed macaque model is an excellent system to investigate the pathogenic mechanisms of HIV infection including both HIV-induced CNS and peripheral nerve damage (Clements et al. 2002; Ebenezer et al. 2009; Haigwood 2004; Laast et al. 2007; Mankowski et al. 2002a, b, 2004; Van Rompay et al. 2006; Zink et al. 2001, 2006). SIV-infected pigtailed macaques rapidly regenerate nerves through collateral sprouting to re-establish normal innervation following excisional skin biopsies. This contrasts with human studies in which we found incomplete collateral sprouting after 2 years. Therefore, the macaque model can accelerate study of human nerve regrowth. In this study, we used a cutaneous excision axotomy macaque model to assess the rate of repair and the relationship between regrowing blood vessels and associated regenerating axons to include the effect of SIV infection on neurovascular repair.

Materials and methods

Animal studies

Six uninfected and five SIV-infected pig-tailed macaques (*Macaca nemestrina*) were evaluated in this study. SIV-infected macaques were simultaneously inoculated with the neurovirulent clone SIV/17E-Fr and the immunosuppressive swarm SIV/DeltaB670. Together, this co-infection recapitulates many of the neuropathological features seen in HIV infection among humans including peripheral nerve damage (Ebenezer et al. 2009; Laast et al. 2007, 2011; Mankowski et al. 2004). The number of circulating CD4+ T cells in the peripheral blood and plasma SIV RNA levels were measured as previously described (Mankowski et al. 2004). The excisional injury was performed using 3 mm diameter cutaneous axotomies along the dorsal interscapular

skin of the back, 2 cm lateral to the spinous processes between T4 and T 10. A single incision was made using a 3-mm circular skin punch (Acupunch™, Acuderm, FL) followed immediately by removal of the incised tissue core, including epidermis and dermis to a depth of 6 mm. Using this technique, epidermal axons were systematically transected to produce a uniform injury from which epidermal nerve fiber and vessel regrowth into the healing wound could be reliably measured. Each incision was located 1 cm caudal to the previous site at the same distance from the dorsal midline. Excisional sites were allowed to heal without sutures or other interventions. A 5-mm concentric circular biopsy punch that overlapped the previous excision punch was used to harvest the healed 3 mm punch sites, yielding samples containing excision sites that were 14 and 70 days post-axotomy. The animal procedures in this study were reviewed and approved by the Institutional Animal Care and Use Committee in accordance with Animal Welfare Act regulations and the USPHS Policy on Humane Care and Use of Laboratory Animals.

Immunohistochemistry and immunofluorescence

Tissue samples were fixed in 2 % paraformaldehyde/lysine/periodate for 24 h, washed in a phosphate buffer and cryoprotected overnight at 4° in 20 % glycerol/0.1 M Sorensen's phosphate buffer. The biopsies were sectioned with a sliding microtome into 50 μM thick frozen vertical free-floating sections for immunostaining. The primary antibodies used were rabbit anti-PGP 9.5 antibody (1:2,000; Chemicon, Temecula, CA) to detect nerve bundles, mouse anti-human CD31 (PECAM; 1:100; BD Pharmingen) to identify blood vessels, rabbit anti-VEGF antibody (1:3000; Millipore, Temecula, CA) and mouse anti-VEGF antibody (1:500; Millipore, Temecula, CA). A rabbit antibody directed against the pericyte marker NG2 chondroitin sulphate proteoglycan (1:1,500; Millipore, Temecula, CA) was used to detect the relationship between newly forming blood vessels and endothelial cells to the extracellular matrix (ECM).

Nonspecific binding of secondary antibodies was blocked with 4 % normal goat serum (1.0 % Triton X-100, 0.5 % nonfat powdered milk in Tris-buffered saline (TBS), pH 7.4). Sections were rinsed in TBS, pH 7.4, and transferred to secondary antibodies. Secondary antibodies included goat anti-rabbit IgG (Vector Laboratories, Burlingame, CA) and goat anti-mouse IgG (Vector Laboratories, Burlingame, CA) were used at 1:100 dilutions in blocking buffer. The sections were incubated with Avidin-Biotin Complex solution (Vector Laboratories, Burlingame, CA). PGP 9.5 stained sections were developed with blue/gray (SG) chromophore. One percent eosin was used as counterstain.

Secondary antibody conjugated to the fluorescent dyes Cy3 goat anti-rabbit IgG (Jackson Immuno Research Laboratories, Inc, West Grove, PA) was used at 1:150 dilution; Alexa-Fluor 488 goat anti-mouse and goat anti-rabbit IgG (Invitrogen, Carlsbad, CA) were used at 1:500 dilution. DRAQ5 (Biostaus Ltd, San Diego, CA) was used for nuclear staining. Fluorescence-labeled sections were mounted in Prolong Gold anti-fade reagent (Invitrogen, Carlsbad, CA) to prevent fluorescent quenching. Fluorescent samples were analyzed using a Zeiss LSM510 confocal imaging system. Images were collected in 1 μm optical Z-series sections and images from individual optical planes and image projections of stacks of serial optical planes were analyzed.

Morphometry

Three sections from each biopsy containing a known fixed fraction of the sample were immunostained. The area of interest was defined as the dermal region extending from the epidermal/dermal junction to a dermal depth of 2,000 μm. Using an ×2.5/0.075 Plan-Neofluor objective of a Zeiss light microscope, the area of interest was marked. With a ×63/1.40 oil Plan-Neofluor objective, the length of blood vessels and dermal nerves growing into the excision site were measured and expressed per cubic millimeters of tissue, using an unbiased stereology Stereo Investigator space ball probe (MBF Bioscience, Williston, VT) (Ebenezer et al. 2011; Mouton et al. 2002; Rojas et al. 2011). Similar methodology was used for epidermal nerve fiber measurements and estimation of epidermal area at the axotomy site. VEGF-positive cells were quantified using the optical fractionator probe of Stereo Investigator (West et al. 1991). All the stereology measurements were obtained using DAT files of Stereo Investigator.

Statistical analysis

Results are reported as median and range. The non-parametric Mann–Whitney test was used to compare groups. Scatter plots with Spearman's correlation coefficients and respective p values were used to present associations between different measures.

Results

Neurovascular growth pattern

The earliest histological response at Day 14 post-axotomy was the emergence of small tufts of CD31-positive capillaries positioned along the lateral excisional margins and at the base of the axotomised site in the dermis. PGP 9.5 was densely expressed on nerve fibers comprising the nerve bundles along the excision margin in the dermis. Blood vessels closely accompanied the collateral axonal sprouts and both sprouting blood vessels and nerves were oriented centripetally towards the denervated zone (Fig. 1a). Blood vessels visualized as small CD31+ clusters located at the base of the denervated zone at Day 14 subsequently extended longitudinally through the collagen towards the papillary dermis. The regenerative axonal bundles from the base of the denervated zone followed sprouting blood vessels and extended from one blood vessel cluster to adjacent clusters through a stepwise, point-to-point growth pattern to reach the papillary dermis (Fig. 1b). By Day 70, the blood vessels had regressed and the surrounding zone of repair was fibrotic (Fig. 1c). Numerous collateral sprouting axons directly entered the re-epithelialized epidermis from the uninjured epidermis just peripheral to the axotomy site, occasionally forming narrow bundles that extended along the basement membrane with thin axons sprouting from these bundles into the superficial layers of the epidermis. By Day 14, regenerating collateral sprouts extended into the denervated epidermal zone (Figs. 1a and 2c) and by Day 70, these collateral fibers had retracted in length and were indistinguishable from nerve fibers outside axotomy zone. The epidermal nerve regrowth pattern has been well documented in detail in our previous studies (Ebenezer et al. 2009, 2011; Hahn et al. 2007).

Neurovascular growth in control macaques

After axotomy, blood vessels showed robust proliferation and regrowth by Day 14 (median, 297/mm^3; range, 216–321) and gradually stabilized and regressed by Day 70 during the healing process (median, 230 mm/mm^3; range, 172–330) (Fig. 1d). Thus, following axotomy, blood vessel regrowth preceded nerve regeneration. The dermal nerve regrowth started slowly at Day 14 (median, 146 mm/mm^3; range, 76–290) and then progressed to a significantly more robust regenerative growth by Day 70 ($p=0.002$; median, 734 mm/mm^3; range, 639–830) (Fig. 2a).

At Day 14, re-innervating fibers in the epidermis consisted predominantly of collateral sprouts (median, 952 mm/mm^3; range, 730–1,205; Fig. 2b) but by Day 70, significantly higher robust growth consisted of both collaterals and regenerative fibers ($p=0.002$; median, 4,220 mm/mm^3; range, 3,530–5,025; Fig. 2b, d), including extensive terminal arborizations of epidermal nerve fibers (Fig. 2d). The epidermis showed significant proliferation of keratinocytes post-axotomy at Day 14 with epidermal thickness reduced ($p=0.002$) by Day 70 and the terminal fibers reorganized to be fitted compactly within the epidermis (Day 14—median, 0.22 mm^2; range, 0.16–0.34; Day 70—median, 0.09 mm^2; range, 0.09–0.13; Fig. 2c). The extent of intra-epidermal nerve fiber
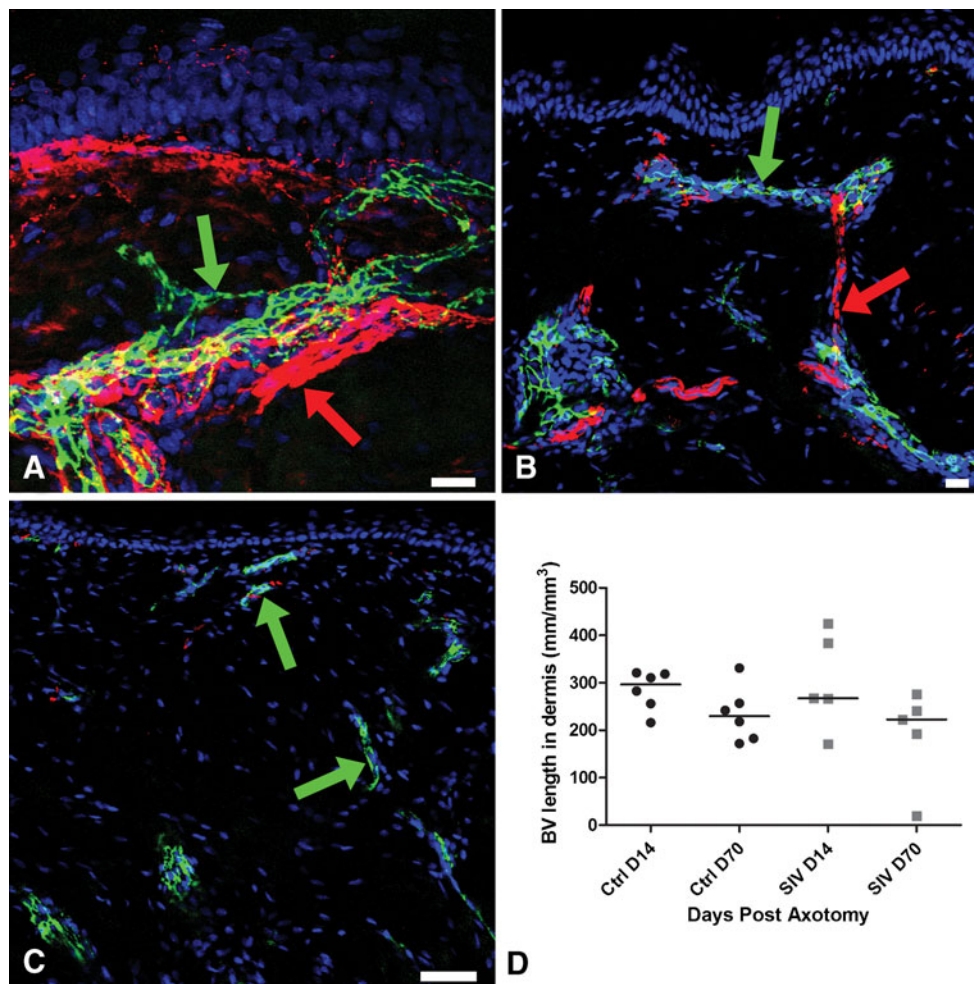
Fig. 1 Growth of blood vessels at the axotomy site, confocal microscopic photographs of post-axotomy sites triple-stained with a neuronal marker (PGP9.5, *red*) a blood vessel marker (CD31, *green*), and a nuclear marker DraQ 5 (*blue*) to characterize the spatiotemporal relationship between blood vessels and nerves during neurovascular regrowth. **a** At Day 14, along the upper lateral excision margin, the blood vessels (CD31: *green arrow*) closely accompany the collateral sprouts of the small axonal bundles (PGP9.5: *red arrow*). Both sprouting blood vessels and collateral nerves are oriented towards the denervated zone. **b** The blood vessels (CD31: *green arrow*) extend longitudinally through the collagenous matrix towards the papillary dermis. The regenerative axonal bundles (PGP9.5: *red arrow*) from the base of the denervated zone extend from one blood vessel cluster to the next. **c** On Day 70, blood vessels are small (CD31: *green arrow*) and the surrounding dermis, the center of the axotomy site, shows dense collagen. **d** Blood vessel growth has regressed by Day 70 post-axotomy with no significant growth difference between uninfected control (*ctrl*) and SIV-infected macaques. *Scale bars*: *A&B*=20 μm; *C*=50 μm

regeneration highly correlated with dermal nerve bundle growth (Spearman's correlation—$r=0.71$, $p=0.01$) and keratinocyte proliferation (Spearman's correlation—$r=-0.85$, $p=<0.001$).

Neurovascular growth in SIV-infected macaques

To determine whether SIV infection altered neurovascular regrowth, we compared vessel and nerve fiber repair in uninfected versus SIV-infected macaques following axotomy. No significant blood vessel growth difference was observed between control and SIV-infected animals (Fig. 1d) at either time point post-axotomy (Day 14—median, 267 mm/mm³; range, 171–425; Day 70—median, 223 mm/mm³; range, 19–276; Fig. 1d).

In contrast with uninfected animals, the SIV-infected macaques exhibited variation in dermal nerve regrowth pattern between animals and failed to show a robust regenerative growth by Day 70 ($p=0.095$, Day 14—median, 215 mm/mm³; range, 76–649; Day 70—median, 524 mm/mm³; range, 438–1,535) in comparison to uninfected macaques (Fig. 2a). The collateral epidermal nerve fibers showed a significant delay at Day 14 ($p=0.01$; median, 310 mm/mm³; range, 91–820), and the regenerative and terminal arborizations also lagged at Day 70 (median, 2,530 mm/mm³; range, 1,446–4,400) (Fig. 2b, e). Decreased epidermal area (median, 0.15 mm²; range, 0.1–0.30 mm²; Fig. 2c) was also observed after injury at Day 70 in both control and SIV-infected macaques.
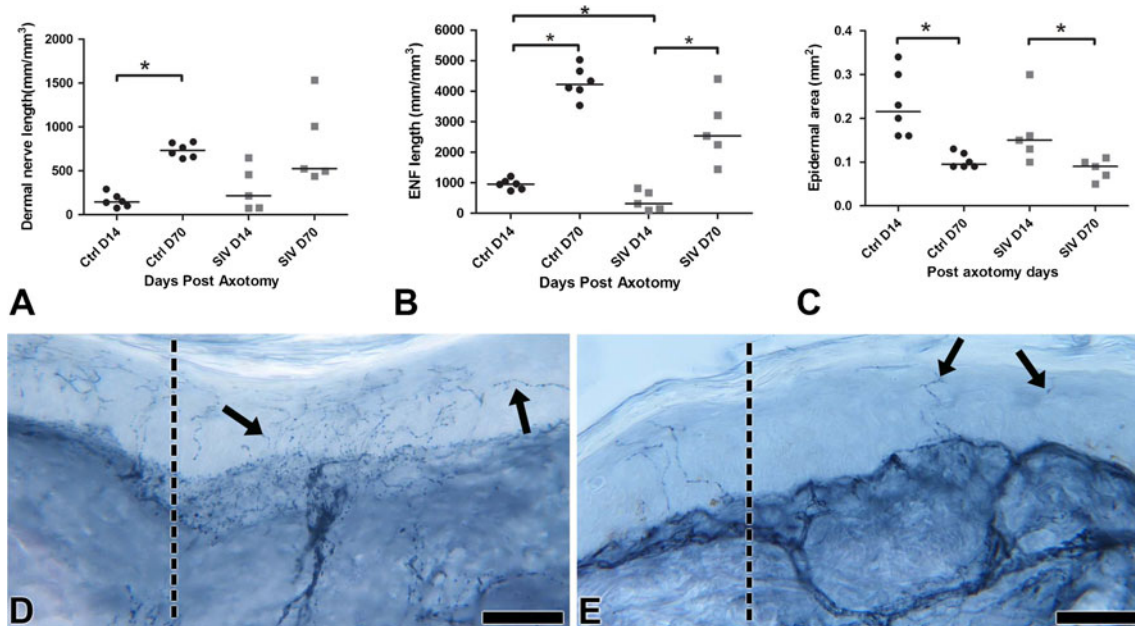
Fig. 2 Growth of cutaneous nerves at the axotomy site. **a** Dermal nerve regrowth in controls (*ctrl*) started slowly at Day 14 but then progressed to robust regenerative growth by Day 70 ($p*=0.002$). In contrast, a more diverse growth pattern was seen between Days 14 to 70 post-axotomy among SIV-infected animals without a significant increase in dermal nerve length at Day 70. **b** In contrast with dermal nerve regrowth, the epidermal nerve fibers showed a significant delay both at Days 14 ($p*=0.01$) and 70 post-axotomy in SIV-infected animals, with decreased regenerative and terminal arborizations. **c** In both controls and SIV-infected animals, epidermal area was significantly reduced at Day 70 after the active regrowth at Day 14 ($p*<0.05$). The epidermis was thinner in SIV-infected animals at Day 14. **d** Day 14 control skin biopsy immunostained for PGP 9.5 showing numerous collaterally sprouting axons (*arrows*) from the excisional margin (*dotted line*) leaning and extending into the denervated epidermis. *Scale bar*=50 μm. **e** Day 14 skin biopsy from an SIV-infected macaque immunostained for PGP 9.5 revealing sparse axons (*arrows*) entering epidermis at the excisional margin (*dotted line*). *Scale bar*=50 μm

Patterns of VEGF expression

Fourteen days following excision, VEGF was expressed along newly formed blood vessel silhouettes at the axotomy site in control macaques. VEGF staining was most prominent on pericytes (Fig. 3a and inset), endothelial cells, and the perivascular cells of the ECM (median, 1,846 cells/mm³; range, 357–3,902; Fig. 3b). The endothelial cells, pericytes and perivascular cells also showed dense expression of NG2, the pericyte marker that co-localized with VEGF (Fig. 3c). Basal keratinocytes in the epidermis showed dense expression of NG2 (Fig. 3d). The number of VEGF-positive cells significantly increased ($p=0.03$; median, 9,856 cells/mm³; range, 1,183–21,959) on Day 70 (Fig. 3b) suggesting that the VEGF expression on pericytes plays a critical role during the vessel maturation period rather than on the earlier phase of vessel sprouting. A strong positive correlation was identified between VEGF expression and extent of dermal nerve regrowth ($r=0.68$, $p=0.01$) and ENF growth ($r=0.63$, $p=0.02$) consistent with cue sharing between these two processes. In addition, VEGF was densely expressed in skin adnexal structures including sweat glands and hair follicles. Although there was a significant increase of VEGF-positive cells in SIV infected animals from Day 14 to Day 70 ($p=$ 0.01), the number of VEGF-positive cells was lower than the uninfected animals at both time points (Day 14—median, 524 cells/mm³; range, 438–1,535; Day 70—median, 4,156 cells/mm³; range, 1,903–14,553; Fig. 3b, d).

A lack of correlation between neurovascular repair markers versus immune status or SIV plasma viral load

To determine whether either immune status or SIV plasma load was associated with alterations in neurovascular repair seen with SIV infection, CD4+ T cell counts (range, 38–1,262 CD+ T cells/μL) and SIV RNA levels in plasma (range, $2.7×10^6$ to $4.9×10^8$ copies/mL) were compared with dermal blood vessel density, dermal nerve fiber length, epidermal nerve fiber length, and number of VEGF-positive cells for both Days 14 and 70 post-axotomy groups. No significant correlations were identified between any neurovascular indices and either CD4+ T cell count or plasma viral load at either time point.

Discussion

This study used a cutaneous excision axotomy model to characterize different components of neurovascular outgrowth
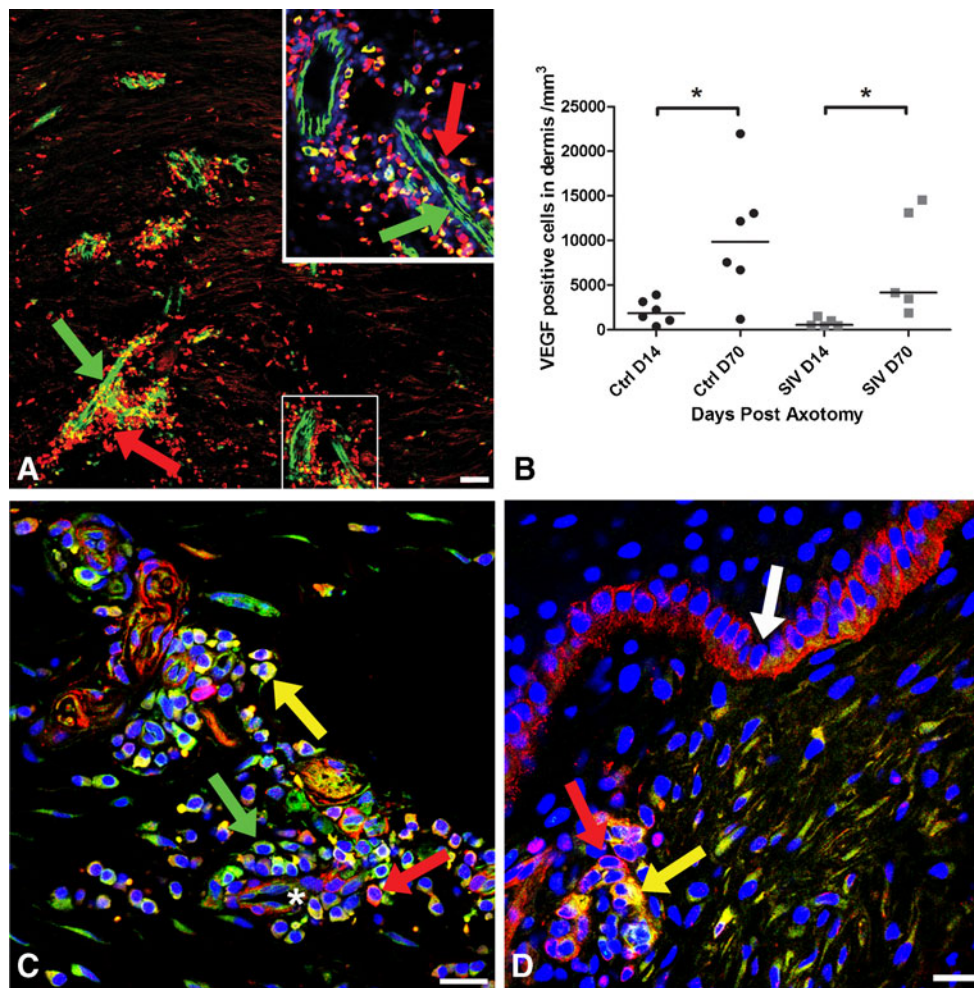
Fig. 3 Localization of VEGF and NG2 expression at the axotomy site. **a** Confocal microscopy montage of a 50-μm section 14 days post-axotomy, triple-stained with the blood vessel marker (CD31: *green*), anti-VEGF-A (*red*) and nuclear marker DraQ 5 (*blue*) to examine the relationship between blood vessels and VEGF expression during regeneration. The base of the axotomy site demonstrates dense expression of VEGF (*red, arrow*) around and along the track of growing blood vessels (*green, arrow*). The area enlarged in *inset* (*upper right*) represents CD31-positive blood vessels (*green*) and numerous closely opposed pericytes and perivascular cells showing dense expression of VEGF (*red*). *Scale bar*=50 μm. **b** The number of VEGF-positive cells significantly increased by Day 70 post-axotomy compared with Day 14 in uninfected animals (p^*=0.03). There was a significant increase of VEGF-positive cells in SIV infected animals from Days 14 to 70 (p^*=0.01), but the number of VEGF-positive cells was lower than the uninfected animals at both time points. **c** Confocal microscopic photograph from 50-μm thick section of skin from a control animal at Day 70 post-axotomy, triple-stained for VEGF-A (*green*), NG2 to stain pericytes (*red*), and nuclear marker DraQ 5 (*blue*) to identify VEGF expression on pericytes during the regeneration process. Neurovascular bundle (*asterisk*) at the base of axotomy site showing pericytes and closely opposed perivascular cells densely expressing VEGF (*green, arrow*) and NG2 (*red, arrow*) exhibiting co-localization (*yellow*). *Scale bar*=10 μm. **d** In contrast to control animals, a Day 14 skin biopsy section from an SIV-infected macaque shows fewer VEGF-positive cells, represented by a small cluster of VEGF expressing cells co-localizing (*yellow, arrow*) with NG2-positive pericytes (*red, arrow*) around a blood vessel at the axotomy site near the epidermis. Basal keratinocytes are positive for NG2 (*white arrow*). *Scale bar*=10 μm

during critical steps of regeneration in both control and SIV-infected macaques. We previously observed that collateral sprouts are the earliest type of nerve fibers to re-innervate the axotomized epidermis and we now report that blood vessels closely accompany regenerating nerves along the excision margin. This relationship is consistent with nerve and blood vessels sharing a common mechanism for regrowth post-axotomy (Bates et al. 2003; Mukouyama et al. 2005, 2002). At the center of the axotomy site, blood vessel regrowth preceded ingrowth of regenerative nerve fibers with blood vessels serving as nidus and scaffolding to guide nerves through the collagen matrix. Earlier studies have shown that axonal extensions were numerous in areas where the blood vessels were oriented longitudinally and neovascularization preceded the axonal extension (Hobson et al. 1997; Waris 1978). Our findings are consistent with experimental reports from other systems, showing the interdependence

of nerves and blood vessels for migration during regeneration (Bates et al. 2003; Gu et al. 2003; Jin et al. 2002; Schwarz et al. 2004) and suggest that promoting vascular growth may facilitate axonal regeneration.

Vascular regrowth after injury supports many repair functions locally at the site of axonal injury including re-establishment of metabolic support and production of trophic growth factors. Vascular growth factors have been shown to be associated with vascular density, orientation and permeability during vascular development (Bates et al. 2003; Drake and Little 1995, 1999; Flamme et al. 1995; Yin and Pacifici 2001). Secretion of VEGF directly influences the recruitment of perineural vascular plexi to nourish developing neural tubes (Aiello et al. 1994) and have been implicated in neuronal patterning, migration, and neural repair (Bates et al. 2003; Hobson et al. 2000; Schwarz et al. 2004; Yu et al. 2008). The increase of VEGF expressing pericytes around neurovascular units at the site of axotomy and its close association with nerve regeneration indicates that VEGF plays a significant role in enhancing cutaneous nerve regeneration.

There is evidence that vascular growth factors promote and sustain neuronal regeneration both by stimulating supporting cells such as astrocytes and Schwann cells, and by enhancing neovascularization (Khaibullina et al. 2004; Krum and Khaibullina 2003; Krum et al. 2008; Sondell et al. 1999; Wang et al. 2005). Microenvironment significantly changes during wound healing and growth factors, ECM and surrounding cells interact to alter the progression of vessel formation. During new vessel sprouting, endothelial cells adhere to each other and form a lumen and then become encircled by a basement membrane and recruited pericytes (Darland et al. 2003; Kuiper et al. 2004; Ozerdem and Stallcup 2003; Virgintino et al. 2007; von Tell et al. 2006). We show that the NG2-rich perivascular cells in the ECM are located along the neurovascular path and densely co-express VEGF during vessel formation and maturation stages. Dense expression of VEGF on pericytes and on NG2-rich perivascular cells is closely associated with nerve regeneration, demonstrating its role in creating a conducive environment for the accompanying nerves to track through the ECM and epidermal basal keratinocytes (de Castro et al. 2005; Kuiper et al. 2004; Ozerdem and Stallcup 2003; Paquet-Fifield et al. 2009; Rezajooi et al. 2004; Virgintino et al. 2007; von Tell et al. 2006). Abundant expression of VEGF on sweat glands and on hair follicles in skin likely provides additional trophic support for regeneration of axons through activation of VEGFR-2 receptor to reach the target (Brown et al. 1992; Detmar et al. 1995; Hobson et al. 1997; Man et al. 2009; Nishimura et al. 2002; Pammer et al. 1998; Sondell et al. 2000).

Impact of SIV infection on neurovascular patterns

Our study shows that SIV infection does not alter the spatiotemporal relationship between regenerative fibers and blood vessels at the dermal level, with no significant defect in blood vessel regrowth. This finding is consistent with a previous report that endothelial adhesion molecule expression is not altered in the peripheral nerve and does not play a critical role in the axonal damage of patients with HIV SN (Fenzi et al. 2006). The contrast between our findings and the extensive neurovascular growth impairment observed in diabetic patients with DPN suggests differences in basic etiological factors modifying neurovascular growth in these sensory neuropathies (Ebenezer et al. 2011). HIV SN patients have shown loss of small sensory nerve fibers, and abnormalities in nerve regeneration have been reported early in HIV infection (Hahn et al. 2007; Holland et al. 1997; Keswani et al. 2003; Polydefkis et al. 2002). We previously observed that SIV infection was associated with altered length, pruning and terminal arborizations of nerve fibers, and the altered nerve growth predominantly was localized to epidermis of the skin. In addition, we reported that Schwann cells expressed low affinity nerve growth factor receptor (p75) enclosing these terminal sensory nerve fibers in skin with impaired nerve regrowth (Ebenezer et al. 2009). Studies indicate proliferating keratinocytes are a major source of nerve growth factors, and growth factors secreted by vessels and nerves in turn influence the growth of epidermal keratinocytes. (Albers and Davis 2007; Brown et al. 1992; Park et al. 2003; Pincelli et al. 1996; Ward et al. 2011). The strong association between epidermal regrowth and neurovascular growth in control animals clearly indicates co-dependent interactions between the vessels and nerves at the cutaneous level during regenerative phases of repair post-axotomy. In contrast, SIV infection may impair the ability of the nerves to regenerate through the dermal ECM because of decreased VEGF expression.

In conclusion, our study demonstrates that the vasculature may influence peripheral nerve regeneration patterns by providing diffusible guidance cues. In particular, local expression of VEGF modulates the surrounding extracellular matrix to generate a favorable environment for axons to regrow. Though SIV infection has no direct effect on vascular growth patterns post-axotomy, impaired nerve terminal regrowth seen with SIV infection may be the result of downregulated VEGF expression, thereby altering the ECM microenvironment that is crucial for guiding regenerating nerve fibers to their targets. The ability to characterize alterations in neurovascular repair post-axotomy in macaques, including those infected with SIV, may guide development of novel therapeutic approaches to promote nerve regeneration.

References

Aiello LP, Avery RL, Arrigg PG, Keyt BA, Jampel HD, Shah ST, Pasquale LR, Thieme H, Iwamoto MA, Park JE et al (1994) Vascular endothelial growth factor in ocular fluid of patients with diabetic retinopathy and other retinal disorders. N Engl J Med 331:1480–1487

Albers KM, Davis BM (2007) The skin as a neurotrophic organ. Neuroscientist 13:371–382

Anton ES, Weskamp G, Reichardt LF, Matthew WD (1994) Nerve growth factor and its low-affinity receptor promote Schwann cell migration. Proc Natl Acad Sci USA 91:2795–2799

Bates DO, Jones RO (2003) The role of vascular endothelial growth factor in wound healing. Int J Low Extrem Wounds 2:107–120

Bates D, Taylor GI, Minichiello J, Farlie P, Cichowitz A, Watson N, Klagsbrun M, Mamluk R, Newgreen DF (2003) Neurovascular congruence results from a shared patterning mechanism that utilizes Semaphorin3A and Neuropilin-1. Dev Biol 255:77–98

Brockington A, Wharton SB, Fernando M, Gelsthorpe CH, Baxter L, Ince PG, Lewis CE, Shaw PJ (2006) Expression of vascular endothelial growth factor and its receptors in the central nervous system in amyotrophic lateral sclerosis. J Neuropathol Exp Neurol 65:26–36

Brown LF, Yeo KT, Berse B, Yeo TK, Senger DR, Dvorak HF, van de Water L (1992) Expression of vascular permeability factor (vascular endothelial growth factor) by epidermal keratinocytes during wound healing. J Exp Med 176:1375–1379

Carmeliet P, Tessier-Lavigne M (2005) Common mechanisms of nerve and blood vessel wiring. Nature 436:193–200

Clements JE, Babas T, Mankowski JL, Suryanarayana K, Piatak M Jr, Tarwater PM, Lifson JD, Zink MC (2002) The central nervous system as a reservoir for simian immunodeficiency virus (SIV): steady-state levels of SIV DNA in brain from acute through asymptomatic infection. J Infect Dis 186:905–913

Darland DC, Massingham LJ, Smith SR, Piek E, Saint-Geniez M, D'Amore PA (2003) Pericyte production of cell-associated VEGF is differentiation-dependent and is associated with endothelial survival. Dev Biol 264:275–288

de Castro R Jr, Tajrishi R, Claros J, Stallcup WB (2005) Differential responses of spinal axons to transection: influence of the NG2 proteoglycan. Exp Neurol 192:299–309

Detmar M, Yeo KT, Nagy JA, Van de Water L, Brown LF, Berse B, Elicker BM, Ledbetter S, Dvorak HF (1995) Keratinocyte-derived vascular permeability factor (vascular endothelial growth factor) is a potent mitogen for dermal microvascular endothelial cells. J Invest Dermatol 105:44–50

Drake CJ, Little CD (1995) Exogenous vascular endothelial growth factor induces malformed and hyperfused vessels during embryonic neovascularization. Proc Natl Acad Sci USA 92:7657–7661

Drake CJ, Little CD (1999) VEGF and vascular fusion: implications for normal and pathological vessels. J Histochem Cytochem 47:1351–1356

Ebenezer GJ, Laast VA, Dearman B, Hauer P, Tarwater PM, Adams RJ, Zink MC, McArthur JC, Mankowski JL (2009) Altered cutaneous nerve regeneration in a simian immunodeficiency virus/macaque intracutaneous axotomy model. J Comp Neurol 514:272–283

Ebenezer GJ, O'Donnell R, Hauer P, Cimino NP, McArthur JC, Polydefkis M (2011) Impaired neurovascular repair in subjects with diabetes following experimental intracutaneous axotomy. Brain 134:1853–1863

Fenzi F, Rossi F, Rava M, Cavallaro T, Ferrari S, Rizzuto N (2006) Endothelial adhesion molecule expression is unaltered in the peripheral nerve from patients with AIDS and distal sensory polyneuropathy. J Neuroimmunol 178:111–116

Ferrara N, Davis-Smyth T (1997) The biology of vascular endothelial growth factor. Endocr Rev 18:4–25

Flamme I, von Reutern M, Drexler HC, Syed-Ali S, Risau W (1995) Overexpression of vascular endothelial growth factor in the avian embryo induces hypervascularization and increased vascular permeability without alterations of embryonic pattern formation. Dev Biol 171:399–414

Gora-Kupilas K, Josko J (2005) The neuroprotective function of vascular endothelial growth factor (VEGF). Folia Neuropathol 43:31–39

Gordon T, Chan KM, Sulaiman OA, Udina E, Amirjani N, Brushart TM (2009) Accelerating axon growth to overcome limitations in functional recovery after peripheral nerve injury. Neurosurgery 65:132–144

Griffin JW, Thompson WJ (2008) Biology and pathology of nonmyelinating Schwann cells. Glia 56:1518–1531

Gu C, Limberg BJ, Whitaker GB, Perman B, Leahy DJ, Rosenbaum JS, Ginty DD, Kolodkin AL (2002) Characterization of neuropilin-1 structural features that confer binding to semaphorin 3A and vascular endothelial growth factor 165. J Biol Chem 277:18069–18076

Gu C, Rodriguez ER, Reimert DV, Shu T, Fritzsch B, Richards LJ, Kolodkin AL, Ginty DD (2003) Neuropilin-1 conveys semaphorin and VEGF signaling during neural and cardiovascular development. Dev Cell 5:45–57

Hahn K, Triolo A, Hauer P, McArthur JC, Polydefkis M (2007) Impaired reinnervation in HIV infection following experimental denervation. Neurology 68:1251–1256

Haigwood NL (2004) Predictive value of primate models for AIDS. AIDS Rev 6:187–198

Hobson MI, Brown R, Green CJ, Terenghi G (1997) Inter-relationships between angiogenesis and nerve regeneration: a histochemical study. Br J Plast Surg 50:125–131

Hobson MI, Green CJ, Terenghi G (2000) VEGF enhances intraneural angiogenesis and improves nerve regeneration after axotomy. J Anat 197(Pt 4):591–605

Holland NR, Stocks A, Hauer P, Cornblath DR, Griffin JW, McArthur JC (1997) Intraepidermal nerve fiber density in patients with painful sensory neuropathy. Neurology 48:708–711

Jin K, Zhu Y, Sun Y, Mao XO, Xie L, Greenberg DA (2002) Vascular endothelial growth factor (VEGF) stimulates neurogenesis in vitro and in vivo. Proc Natl Acad Sci USA 99:11946–11950

Keswani SC, Polley M, Pardo CA, Griffin JW, McArthur JC, Hoke A (2003) Schwann cell chemokine receptors mediate HIV-1 gp120 toxicity to sensory neurons. Ann Neurol 54:287–296

Khaibullina AA, Rosenstein JM, Krum JM (2004) Vascular endothelial growth factor promotes neurite maturation in primary CNS neuronal cultures. Brain Res Dev Brain Res 148:59–68

Krum JM, Khaibullina A (2003) Inhibition of endogenous VEGF impedes revascularization and astroglial proliferation: roles for VEGF in brain repair. Exp Neurol 181:241–257

Krum JM, Mani N, Rosenstein JM (2008) Roles of the endogenous VEGF receptors flt-1 and flk-1 in astroglial and vascular remodeling after brain injury. Exp Neurol 212:108–117

Kuiper EJ, Witmer AN, Klaassen I, Oliver N, Goldschmeding R, Schlingemann RO (2004) Differential expression of connective tissue growth factor in microglia and pericytes in the human diabetic retina. Br J Ophthalmol 88:1082–1087

Laast VA, Pardo CA, Tarwater PM, Queen SE, Reinhart TA, Ghosh M, Adams RJ, Zink MC, Mankowski JL (2007) Pathogenesis of simian immunodeficiency virus-induced alterations in macaque trigeminal ganglia. J Neuropathol Exp Neurol 66:26–34

Laast V, Shim B, Johanek L, Dorsey J, Hauer P, Tarwater P, Pardo C, McArthur J, Ringkamp M, Mankowski J (2011) Macrophage-mediated dorsal root ganglion damage precedes altered nerve conduction in SIV-infected macaques. Am J Pathol 179:2337–2345

Man XY, Yang XH, Cai SQ, Bu ZY, Wu XJ, Lu ZF, Zheng M (2009) Expression and localization of vascular endothelial growth factor and vascular endothelial growth factor receptor-2 in human epidermal appendages: a comparison study by immunofluorescence. Clin Exp Dermatol 34:396–401

Mankowski JL, Clements JE, Zink MC (2002a) Searching for clues: tracking the pathogenesis of human immunodeficiency virus central nervous system disease by use of an accelerated, consistent simian immunodeficiency virus macaque model. J Infect Dis 186(Suppl 2):S199–S208

Mankowski JL, Queen SE, Tarwater PM, Fox KJ, Perry VH (2002b) Accumulation of beta-amyloid precursor protein in axons correlates with CNS expression of SIV gp41. J Neuropathol Exp Neurol 61:85–90

Mankowski JL, Queen SE, Clements JE, Zink MC (2004) Cerebrospinal fluid markers that predict SIV CNS disease. J Neuroimmunol 157:66–70

Mouton PR, Gokhale AM, Ward NL, West MJ (2002) Stereological length estimation using spherical probes. J Microsc 206:54–64

Mukouyama YS, Shin D, Britsch S, Taniguchi M, Anderson DJ (2002) Sensory nerves determine the pattern of arterial differentiation and blood vessel branching in the skin. Cell 109:693–705

Mukouyama YS, Gerber HP, Ferrara N, Gu C, Anderson DJ (2005) Peripheral nerve-derived VEGF promotes arterial differentiation via neuropilin 1-mediated positive feedback. Development 132:941–952

Navarro X, Vivo M, Valero-Cabre A (2007) Neural plasticity after peripheral nerve injury and regeneration. Prog Neurobiol 82:163–201

Nishimura S, Maeno N, Matsuo K, Nakajima T, Kitajima I, Saito H, Maruyama I (2002) Human lactiferous mammary gland cells produce vascular endothelial growth factor (VEGF) and express the VEGF receptors, Flt-1 AND KDR/Flk-1. Cytokine 18:191–198

Ozerdem U, Stallcup WB (2003) Early contribution of pericytes to angiogenic sprouting and tube formation. Angiogenesis 6:241–249

Pammer J, Weninger W, Mildner M, Burian M, Wojta J, Tschachler E (1998) Vascular endothelial growth factor is constitutively expressed in normal human salivary glands and is secreted in the saliva of healthy individuals. J Pathol 186:186–191

Paquet-Fifield S, Schluter H, Li A, Aitken T, Gangatirkar P, Blashki D, Koelmeyer R, Pouliot N, Palatsides M, Ellis S, Brouard N, Zannettino A, Saunders N, Thompson N, Li J, Kaur P (2009) A role for pericytes as microenvironmental regulators of human skin tissue regeneration. J Clin Invest 119:2795–2806

Park JA, Choi KS, Kim SY, Kim KW (2003) Coordinated interaction of the vascular and nervous systems: from molecule- to cell-based approaches. Biochem Biophys Res Commun 311:247–253

Pincelli C, Fantini F, Giannetti A (1996) Neuropeptides, nerve growth factor and the skin. Pathol Biol (Paris) 44:856–859

Polydefkis M, Yiannoutsos CT, Cohen BA, Hollander H, Schifitto G, Clifford DB, Simpson DM, Katzenstein D, Shriver S, Hauer P, Brown A, Haidich AB, Moo L, McArthur JC (2002) Reduced intraepidermal nerve fiber density in HIV-associated sensory neuropathy. Neurology 58:115–119

Rajan B, Polydefkis M, Hauer P, Griffin JW, McArthur JC (2003) Epidermal reinnervation after intracutaneous axotomy in man. J Comp Neurol 457:24–36

Rezajooi K, Pavlides M, Winterbottom J, Stallcup WB, Hamlyn PJ, Lieberman AR, Anderson PN (2004) NG2 proteoglycan expression in the peripheral nervous system: upregulation following injury and comparison with CNS lesions. Mol Cell Neurosci 25:572–584

Rojas C, Stathis M, Polydefkis M, Rudek MA, Zhao M, Ebenezer GJ, Slusher BS (2011) Glutamate carboxypeptidase activity in human skin biopsies as a pharmacodynamic marker for clinical studies. J Transl Med 9:27

Saxena S, Caroni P (2007) Mechanisms of axon degeneration: from development to disease. Prog Neurobiol 83:174–191

Schwarz Q, Gu C, Fujisawa H, Sabelko K, Gertsenstein M, Nagy A, Taniguchi M, Kolodkin AL, Ginty DD, Shima DT, Ruhrberg C (2004) Vascular endothelial growth factor controls neuronal migration and cooperates with Sema3A to pattern distinct compartments of the facial nerve. Genes Dev 18:2822–2834

Soker S, Miao HQ, Nomi M, Takashima S, Klagsbrun M (2002) VEGF165 mediates formation of complexes containing VEGFR-2 and neuropilin-1 that enhance VEGF165-receptor binding. J Cell Biochem 85:357–368

Sondell M, Lundborg G, Kanje M (1999) Vascular endothelial growth factor stimulates Schwann cell invasion and neovascularization of acellular nerve grafts. Brain Res 846:219–228

Sondell M, Sundler F, Kanje M (2000) Vascular endothelial growth factor is a neurotrophic factor which stimulates axonal outgrowth through the flk-1 receptor. Eur J Neurosci 12:4243–4254

Song XY, Zhou FH, Zhong JH, Wu LL, Zhou XF (2006) Knockout of p75(NTR) impairs re-myelination of injured sciatic nerve in mice. J Neurochem 96:833–842

Terenghi G (1999) Peripheral nerve regeneration and neurotrophic factors. J Anat 194(Pt 1):1–14

Van Rompay KK, Singh RP, Heneine W, Johnson JA, Montefiori DC, Bischofberger N, Marthas ML (2006) Structured treatment interruptions with tenofovir monotherapy for simian immunodeficiency virus-infected newborn macaques. J Virol 80:6399–6410

Virgintino D, Girolamo F, Errede M, Capobianco C, Robertson D, Stallcup WB, Perris R, Roncali L (2007) An intimate interplay between precocious, migrating pericytes and endothelial cells governs human fetal brain angiogenesis. Angiogenesis 10:35–45

von Tell D, Armulik A, Betsholtz C (2006) Pericytes and vascular stability. Exp Cell Res 312:623–629

Wang WY, Dong JH, Liu X, Wang Y, Ying GX, Ni ZM, Zhou CF (2005) Vascular endothelial growth factor and its receptor Flk-1 are expressed in the hippocampus following entorhinal deafferentation. Neuroscience 134:1167–1178

Ward NL, Hatala DA, Wolfram JA, Knutsen DA, Loyd CM (2011) Cutaneous manipulation of vascular growth factors leads to alterations in immunocytes, blood vessels and nerves: evidence for a cutaneous neurovascular unit. J Dermatol Sci 61:14–22

Waris T (1978) Innervation of scar tissue in the skin of the rat. Scand J Plast Reconstr Surg 12:173–180

West MJ, Slomianka L, Gundersen HJ (1991) Unbiased stereological estimation of the total number of neurons in thesubdivisions of the rat hippocampus using the optical fractionator. Anat Rec 231:482–497

Yin M, Pacifici M (2001) Vascular regression is required for mesenchymal condensation and chondrogenesis in the developing limb. Dev Dyn 222:522–533

Yu CQ, Zhang M, Matis KI, Kim C, Rosenblatt MI (2008) Vascular endothelial growth factor mediates corneal nerve repair. Invest Ophthalmol Vis Sci 49:3870–3878

Zink MC, Coleman GD, Mankowski JL, Adams RJ, Tarwater PM, Fox K, Clements JE (2001) Increased macrophage chemoattractant protein-1 in cerebrospinal fluid precedes and predicts simian immunodeficiency virus encephalitis. J Infect Dis 184:1015–1021

Zink MC, Laast VA, Helke KL, Brice AK, Barber SA, Clements JE, Mankowski JL (2006) From mice to macaques—animal models of HIV nervous system disease. Curr HIV Res 4:293–305